The build-up and relaxation of stresses in a glass-forming soft-sphere mixture under shear: A computer simulation study

A Letters Journal Exploring the Frontiers of Physics

December 2009

EPL, **88** (2009) 60001
doi: 10.1209/0295-5075/88/60001

www.epljournal.org

The build-up and relaxation of stresses in a glass-forming soft-sphere mixture under shear: A computer simulation study

J. Zausch[1(a)] and J. Horbach[2(b)]

[1] *Institut für Physik, Johannes Gutenberg-Universität Mainz - Staudinger Weg 7, D-55099 Mainz, Germany, EU*
[2] *Institut für Materialphysik im Weltraum, Deutsches Zentrum für Luft- und Raumfahrt (DLR) 51170 Köln, Germany, EU*

received 4 November 2009; accepted in final form 27 November 2009
published online 17 December 2009

PACS 05.70.Ln – Nonequilibrium and irreversible thermodynamics
PACS 47.50.Cd – Non-Newtonian fluid flows: Modeling
PACS 83.60.Rs – Shear rate-dependent structure (shear thinning and shear thickening)

Abstract – Molecular-dynamics computer simulations in conjunction with Lees-Edwards boundary conditions are used to investigate a glass-forming binary Yukawa fluid under shear. The transition from the elastic response to plastic flow is elucidated by studying the stress relaxation after switching off the shear. We find a slow stress relaxation starting from states in the elastic regime and a fast one starting from states in the plastic-flow regime. We show that these relaxation patterns are related to a different distribution of local microscopic stresses in both cases.

Introduction. – The rheological behavior of soft-glassy materials as well as of metallic glasses is of great technological importance and provides a very rich phenomenology [1,2]. If shear flow is imposed on a glass-forming fluid at a constant shear rate $\dot{\gamma}$, a constant steady-state stress σ is built up that strongly affects relaxation processes in the fluid. An ubiquitous phenomenon is known as shear thinning, *i.e.* a decrease of the effective shear viscosity $\eta_{\rm eff} = \sigma/\dot{\gamma}$ with increasing $\dot{\gamma}$. Whereas for $\dot{\gamma} \to 0$ the effective shear viscosity $\eta_{\rm eff}$ approaches the equilibrium shear viscosity η, in glass-forming fluids $\eta_{\rm eff}$ can be orders of magnitude smaller than η (see, *e.g.*, the recent experiment of colloidal hard spheres by Besseling *et al.* [3]).

To reveal non-linear phenomena such as shear thinning, it is crucial to understand the transition of a glass-forming fluid from its quiescent state towards the final steady-state flow. After switching on shear, there is first a regime of "elastic response", followed by a transition towards plastic flow in the steady state. Recently, different approaches have been used to understand the latter transition on a microscopic level: On the one hand, the transition to plastic flow has been described in terms of local irreversible events (similar to dislocations in crystalline solids) that exhibit a quadrupolar symmetry (see, *e.g.*, refs. [4–6]). These local events have been also referred to as shear transformation zones [7]. On the other hand, the mode coupling theory (MCT) for sheared glassy systems [8–12] has been proven successful to describe various aspects of the non-linear response of glass-forming systems to shear, such as shear thinning [13–18], the existence of a yield stress in glasses [19–24], the fluctuation-dissipation theorem for sheared systems [15–17,25], and the occurrence of a transient superdiffusive regime in the mean-squared displacement [26]. However, MCT does not include a description in terms of local properties or inhomogeneities such as shear transformation zones.

In this letter, non-equilibrium molecular-dynamics (MD) computer simulations of a sheared glass-forming soft-sphere mixture are used to investigate the interplay between local and macroscopic stresses in the elastic-response regime and in the plastic-flow regime. Our aim is to shed light on the relation between a description in terms of local irreversible events and theories such as MCT that provide a microscopic description in terms of average properties.

We first show that the identification of changes in the average structure (to leading order on a pair correlation level) is not appropriate to distinguish a state in the regime of elastic response from one in the plastic-flow regime. However, a very different behavior in the latter two regimes is observed with respect to the relaxation of

(a) Present address: Fraunhofer Institut für Techno- und Wirtschaftsmathematik (ITWM) - Fraunhofer-Platz 1, 67663 Kaiserslautern, Germany, EU.
(b) E-mail: juergen.horbach@dlr.de

stresses when suddenly switching off the shear. Whereas from states in the elastic regime, stresses relax slowly on the typical relaxation time scale of the unsheared system, from states in the plastic-flow regime, a rapid relaxation on the time scale $1/\dot{\gamma}$ is seen. This behavior can be understood by considering the fluctuations of local stresses that indicate that the transition from an elastic response to the plastic-flow regime is associated with a sudden increase of local stress fluctuations, while the decay of the stress fluctuations is slow when switching off shear in the steady-state regime (in the elastic regime the fluctuations are identical to those at equilibrium). Our results reflect the non-linear shear response of a deeply supercooled liquid. We note that, far below the glass transition temperature of our simulation, also a shear stress relaxation on the time scale $1/\dot{\gamma}$ is observed for the switch-off case. But in this case, instead of decaying to zero, a decay onto a plateau is seen [27].

Our study shows that a state in the elastic-response regime can be distinguished from one in the plastic-flow regime via *local* stress fluctuations. As a characteristic signature of these local fluctuations in average properties, we have identified the decay of the macroscopic shear stress on the time scale $1/\dot{\gamma}$, after switching off the shear stress in the steady state. Thus, although local stress fluctuations are not directly incorporated into MCT, it could be checked whether MCT or similar microscopic theories are able to reproduce the latter relaxation patterns seen in the decay of stresses.

Details of the simulation. – MD simulations were performed for a binary AB mixture under shear. The particles interact via Yukawa potentials, $V_{\alpha\beta}(r) = \varepsilon_{\alpha\beta} d_{\alpha\beta} \exp[-\kappa(r - d_{\alpha\beta})]/r$, with r the distance between particles of type α and β ($\alpha, \beta = \mathrm{A}, \mathrm{B}$). The "particle diameters" are set to $d_{\mathrm{AB}} = 1.1\, d_{\mathrm{AA}}$, $d_{\mathrm{BB}} = 1.2\, d_{\mathrm{AA}}$, the energy parameters to $\varepsilon_{\mathrm{AB}} = 1.4\, \varepsilon_{\mathrm{AA}}$, $\varepsilon_{\mathrm{BB}} = 2.0\, \varepsilon_{\mathrm{AA}}$, and the screening parameter to $\kappa_{\mathrm{AA}} = \kappa_{\mathrm{BB}} = \kappa_{\mathrm{AB}} = 6/d_{\mathrm{AA}}$. For the masses, $m_{\mathrm{A}} = m_{\mathrm{B}} = 1.0$ is chosen. The potentials are truncated at $r_{\mathrm{c}}^{\alpha\beta}$, given by $V_{\alpha\beta}(r_{\mathrm{c}}^{\alpha\beta}) = 10^{-7}\, \epsilon_{\mathrm{AA}}$.

The simulations were done for a $50:50$ mixture of $N = 2N_{\mathrm{A}} = 2N_{\mathrm{B}} = 1600$ particles, placed in a cubic simulation box of linear size $L = 13.3\, d_{\mathrm{AA}}$ (corresponding to a density of $\varrho = 0.675\, m_{\mathrm{A}}/d_{\mathrm{AA}}^3$). For the sheared system, we chose the x-direction as the direction of shear and the y- and z-direction as the gradient and vorticity direction, respectively. Shear was imposed onto the system via modified periodic boundary conditions (Lees-Edwards boundary conditions [28]). After a short time, *i.e.* long before the steady-state regime is approached, this leads to a linear shear profile [26].

Both in equilibrium and under shear, the system is coupled to a dissipative particle dynamics (DPD) thermostat [29]. The details about the parameters used for the DPD thermostat can be found in ref. [26]. The equations of motion were integrated via a generalized form of the velocity Verlet algorithm that has been recently proposed by Peters [30]. For the time step of the integration we used $\delta t = 0.0083\, \tau$ (with the time unit $\tau = \sqrt{m_{\mathrm{A}} d_{\mathrm{AA}}^2/\epsilon_{\mathrm{AA}}}$). First, independent samples were fully equilibrated in the temperature range $1.0 \geqslant T \geqslant 0.14$, performing at least 30 independent runs at each temperature. Below, we present results for the lowest temperature $T = 0.14$ (corresponding to the critical temperature of MCT for our system [27]). In this case, 250 independent runs were done, each of them over 40 million time steps. As a result, 250 equilibrated configurations were obtained that served as starting configurations for production runs at the constant shear rate $\dot{\gamma} = 0.003$. Here, we study the transient dynamics from equilibrium to steady state (*i.e.* after the switch-on of shear) as well as the relaxation dynamics after the cessation of shear. We refer to these simulations as the switch-on and the switch-off case, respectively.

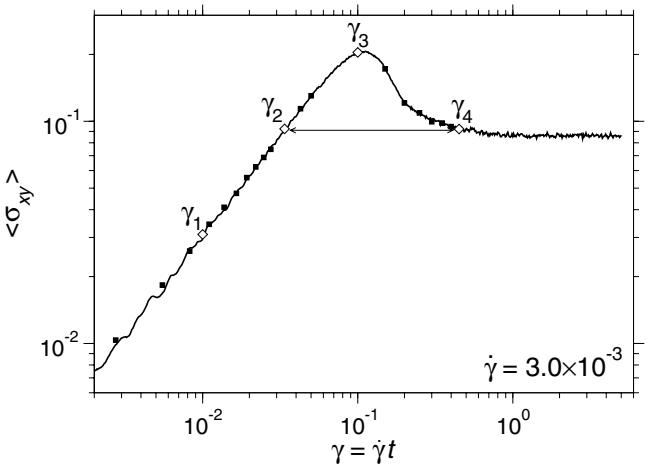

Fig. 1: Stress-strain relation after switching on the shear field with constant shear rate $\dot{\gamma} = 3 \times 10^{-3}$ at time $t = 0$, as computed from eq. (1) (solid line) and from eq. (2) (symbols).

Results. – After the switch-on of the shear, stresses are built up that can be measured by the xy-component of the stress tensor [31],

$$\langle \sigma_{xy} \rangle = \frac{1}{V} \Big\langle \sum_{i=1}^{N} [-m_i v_{i,x} v_{i,y} - \sum_{j>i} r_{ij,x} F_{ij,y}] \Big\rangle, \quad (1)$$

with V the volume, m_j the mass of particle j, $v_{j,x}$ and $v_{j,y}$ respectively the x- and y-component of the velocity of particle j, $r_{ij,x}$ the x-component of the distance and $F_{ij,y}$ the y-component of force between particles i and j.

The averaged shear stress, $\langle \sigma_{xy} \rangle$, as a function of the strain $\gamma = \dot{\gamma} t$ is shown in fig. 1. For $\gamma < 0.1$, $\langle \sigma_{xy} \rangle$ increases almost linearly in time. This early regime indicates an elastic response of the fluid to the external shear field. At a strain $\gamma \approx 1$ (corresponding to a time scale of $1/\dot{\gamma}$), the asymptotic steady-state value of $\langle \sigma_{xy} \rangle$ is reached where the system keeps flowing at a fixed rate. Between the elastic and the plastic regime, the stress exhibits a maximum, $\sigma_{\max}$, at $\gamma \approx 0.1$ marking the transition between the two regimes.

The configurational part of the shear stress can be also calculated from the structural pair correlations via [32,33]

$$\langle\sigma_{xy}\rangle = -\frac{\rho^2}{4}\sqrt{\frac{32\pi}{15}}\sum_{\alpha\beta}\frac{N_\alpha N_\beta}{N^2}\int_0^\infty \mathrm{d}r r^3\frac{\partial V_{\alpha\beta}}{\partial r}\mathrm{Im}\, g_{22}^{\alpha\beta}(r), \tag{2}$$

where $\mathrm{Im}\, g_{22}(r)$ is the imaginary part of the pair correlation function projected onto the spherical harmonic function Y_{22} [34]. This function is a coefficient in the expansion of the pair correlation function [31] $g_{\alpha\beta}(\vec{r})$ into spherical harmonics, $g_{\alpha\beta}(\vec{r}) = \sum_{l=0}^{\infty}\sum_{m=-l}^{l} g_{lm}^{\alpha\beta} Y_{lm}(\theta,\phi)$ (with $Y_{lm}(\theta,\phi)$ the spherical harmonic of degree l and order m of the spherical coordinates θ and ϕ). The functions $g_{lm}^{\alpha\beta}(r)$ are defined by

$$g_{lm}^{\alpha\beta}(r) = \frac{2V}{N_\alpha N_\beta}\left\langle\sum_{i=1}^{N_\alpha}\sum_{j>i}^{N_\beta}\frac{\delta(|\vec{r}_i^{\,\alpha}-\vec{r}_j^{\,\beta}|-r)}{r^2}\,Y_{lm}^*\right\rangle \tag{3}$$

with $\alpha,\beta = \{\mathrm{A},\mathrm{B}\}$, and $\vec{r}_i^{\,\alpha} \equiv (x_i^\alpha, y_i^\alpha, z_i^\alpha)$ the position vector of particle i of type α. Thus, with $\mathrm{Im}\, Y_{22}$ in Cartesian coordinates, $\mathrm{Im}\, Y_{22} = \sqrt{15/(8\pi)}\, xy/r^2$, the function $\mathrm{Im}\, g_{22}^{\alpha\beta}(r)$ is given by

$$\mathrm{Im}\, g_{22}^{\alpha\beta}(r) = \sqrt{\frac{15}{2\pi}}\frac{V}{N_\alpha N_\beta}\left\langle\sum_{i=1}^{N_\alpha}\sum_{j>i}^{N_\beta}\delta(|\vec{r}_i^{\,\alpha}-\vec{r}_j^{\,\beta}|-r) \times\frac{(x_i^\alpha - x_j^\beta)(y_i^\alpha - y_j^\beta)}{r^4}\right\rangle. \tag{4}$$

Below, we also show the function $\mathrm{Re}\, g_{44}^{\alpha\beta}(r)$. This function is the only one of degree $l=4$ that is non-zero for our sheared system in Couette flow geometry [27]. Note that the antisymmetry of the spherical harmonics implies that the $g_{lm}^{\alpha\beta}$ with odd values of l vanish. In the absence of shear, all coefficients except for $g_{00}^{\alpha\beta}$ are zero because then $g_{\alpha\beta}(\vec{r})$ does not exhibit any angular dependence.

In eq. (2) we have omitted the kinetic part since it gives only a minor contribution to $\langle\sigma_{xy}\rangle$. This can be inferred from fig. 1 where the symbols represent the shear stress, as obtained from eq. (2). These symbols are on top of the straight line, that corresponds to $\langle\sigma_{xy}\rangle$, as calculated from eq. (1), including the kinetic part.

The function $\mathrm{Im}\, g_{22}(r)$ is shown in fig. 2(a) for the BB correlations (the AB and AA correlations exhibit similar features and are thus not shown here). Different strains $\gamma_1 = 0.01$, $\gamma_2 = 0.034$, $\gamma_3 = 0.1$ and $\gamma_4 = 0.45$ (before and after the stress overshoot) are displayed. For $\gamma > 0$, pronounced oscillations develop that seem to grow homogeneously on all length scales. In particular, at equal stresses before and after the maximum stress $\sigma_{\max}$ (at the strains γ_2 and γ_4, respectively), the functions $\mathrm{Im}\, g_{22}(r)$ lie on top of each other. This is further illustrated in the inset of fig. 2. Here, the peak value $H_i(\gamma)$ corresponds to the maximum of the i-th peak in $\mathrm{Im}\, g_{22}(r)$. The amplitudes $H_i(\gamma)$ are rescaled such that the maximal amplitude,

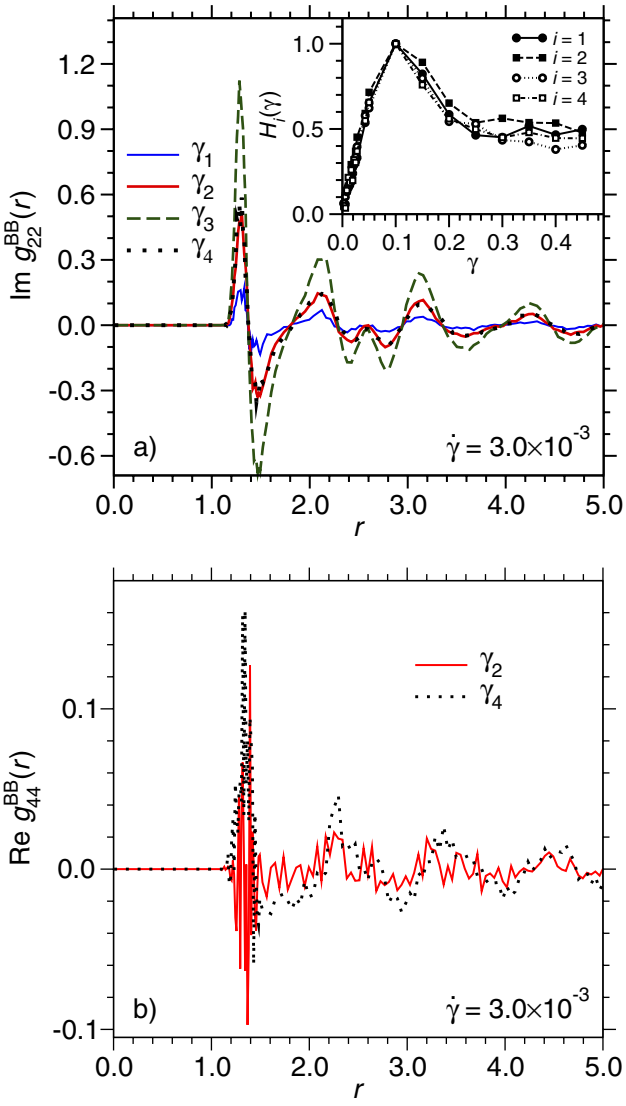

Fig. 2: (Colour on-line) a) $\mathrm{Im}\, g_{22}^{\mathrm{BB}}(r)$ for the BB correlations for the different strains, marked in fig. 1. The inset shows the time dependence of the rescaled height $H_i(\gamma)$ of the i-th maximum in $\mathrm{Im}\, g_{22}(r)$ (see text). b) $\mathrm{Re}\, g_{44}^{\mathrm{BB}}(r)$ for the BB correlations at the strains γ_2 and γ_4 from fig. 1.

attained at $\gamma \approx 0.1$, has a value of 1. In this representation, the different $H_i(\gamma)$ match rather well within the error bars. Thus, with respect to the average structure, as represented by $\mathrm{Im}\, g_{22}(r)$, one cannot distinguish a configuration in the elastic regime from one in the plastic-flow regime, provided the total shear stress of both configurations is equal.

In fig. 2(b), the function $\mathrm{Re}\, g_{44}^{\mathrm{BB}}(r)$ is displayed at the strains γ_2 and γ_4. As the only non-vanishing contribution for $l=4$, the amplitude of the first peak in $\mathrm{Re}\, g_{44}^{\mathrm{BB}}(r)$ is about a factor of 5 lower than that of $\mathrm{Im}\, g_{22}^{\mathrm{BB}}(r)$ at the corresponding values of γ. Different from the behavior of $\mathrm{Im}\, g_{22}^{\mathrm{BB}}$ it seems that the amplitudes of the peaks in $\mathrm{Re}\, g_{44}^{\mathrm{BB}}(r)$ at γ_2 are lower than the ones at γ_4. However, the low signal-to-noise ratio does not allow a final conclusion whether the behavior of $\mathrm{Re}\, g_{44}$

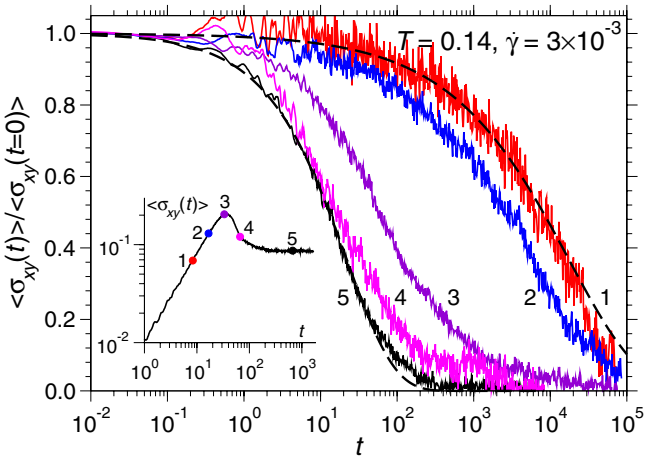

Fig. 3: (Colour on-line) Relaxation of the shear stress, normalized to its initial value, after switching off the shear at the states that are indicated in the inset by symbols and numbers. The dashed lines are fits with Kohlrausch functions (see text).

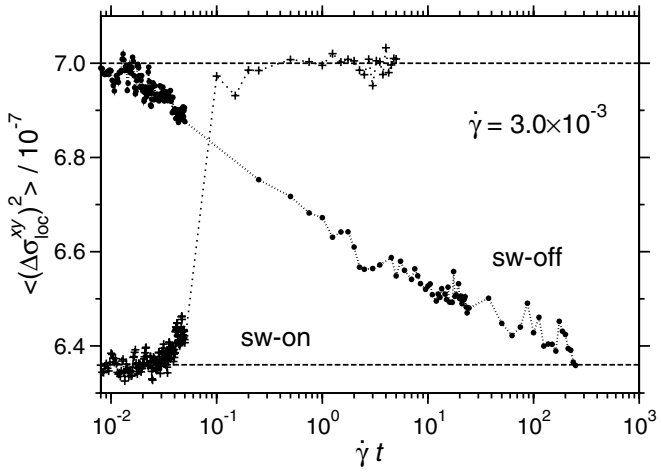

Fig. 4: Time dependence of $\langle(\Delta\sigma^{xy}_{\rm loc})^2\rangle$ for the transition from equilibrium to steady state ("sw-on") and for the transition from steady state towards equilibrium ("sw-off").

is qualitatively different from that of $\mathrm{Im}\, g_{22}$. But with regard to the very small contribution of $\mathrm{Re}\, g_{44}$ in the spherical harmonics expansion of $g(\vec{r})$ one can conclude that to a good approximation the same average structure is obtained at equal stresses. This behavior is different from the one observed in computer simulations of normal liquids [32,33] where, due to the application of large shear rates the function $\mathrm{Re}\, g_{44}$ has a much larger amplitude than in our case. Thus, in the supercooled state (considered here) the application of relatively small shear rates leads to a drastic change of the dynamics while the structural arrangement of particles is only weakly deformed.

The stress relaxation after suddenly switching off the shear depends strongly on whether a state before or after the stress maximum is considered as the initial state. Figure 3 shows the normalized stress $\langle\sigma_{xy}(t)\rangle/\langle\sigma_{xy}(0)\rangle$ for the switch-off case, starting from states that were taken at different times during the transition from equilibrium to steady state (as indicated in the inset). Whereas from the steady state (curve 5), the stress decays on the time scale $1/\dot{\gamma}$, from states before the occurrence of $\sigma_{\rm max}$ (curves 1 and 2), the stresses relax to zero on the two and a half orders of magnitude slower time scale of 10^5 which is comparable to the typical relaxation time of the unsheared system at equilibrium, $\tau_{\rm eq}$ [27]. The dashed lines in fig. 3 are fits with Kohlrausch-Williams-Watts (KWW) functions, $f(t) \propto \exp[-(t/\tau)^\beta]$, yielding $\beta = 0.7$ for the decay from the steady state (curve 5) and $\beta = 0.47$ for the decay from a state in the elastic regime (curve 1).

At this point, we have encountered puzzling features: First, at equal stresses the average structure of a state in the elastic regime can hardly be distinguished from one in the plastic-flow regime, at least on a pair correlation level. We mention that also for the switch-off case a "homogeneous decay" of $\mathrm{Im}\, g_{22}(r)$ is observed such that this function is equal to those for the switch-on case for corresponding equal stresses [27]. Second, for the switch-off case from states in the elastic regime a slow stress relaxation on a time scale comparable to the typical relaxation time of the unsheared system is observed, whereas the stress relaxation starting from states in the steady state occurs on the relatively fast time scale $1/\dot{\gamma}$.

This poses the question how the stress relaxation for the different switch-off cases can be related to changes in static properties when the system undergoes a transition from a solid-like elastic deformation to a plastic-flow state. Since average properties such as the average structure do not seem to describe these differences, it is natural to assume that fluctuations around the average are the key to understand them.

A simple quantity that measures the fluctuations around the average can be extracted from the distribution of the *local* shear stress $\sigma^{xy}_{{\rm loc},i}$, exerted on a single particle. Since the kinetic part of the stress tensor (1) can be neglected, the local shear stress on a particle i can be defined as $\sigma^{xy}_{{\rm loc},i} = -\frac{1}{V}\sum_{j\neq i}^{N} r_{ij,x}F_{ij,y}$. To quantify the fluctuations with respect to this variable, we have determined $\langle(\Delta\sigma^{xy}_{\rm loc})^2\rangle = \langle(\sigma^{xy}_{{\rm loc},i})^2\rangle - \langle(\sigma^{xy}_{{\rm loc},i})\rangle^2$. The latter quantity is displayed in fig. 4 for the switch-on and the switch-off case (note that similar quantities have been considered in the context of foams under shear [35]). For the switch-on case, a rapid increase towards the steady value is seen, occurring around the location of the stress maximum $\sigma_{\rm max}$ (*i.e.* at $\gamma \approx 0.1$). But for the switch-off case, there is a slow relaxation on the time scale $\tau_{\rm eq}$ from the steady-state value to zero.

Now we can understand the different manner in which the stresses relax before and after the stress maximum. Before $\sigma_{\rm max}$ is reached, the width of the stress distribution is the same as in equilibrium, therefore the shear stress decays on the time scale of the equilibrium relaxation. At times after the appearance of $\sigma_{\rm max}$, the "long-living" higher stress fluctuations support a rapid decay of the average shear stress. The behavior of $\langle(\Delta\sigma^{xy}_{\rm loc})^2\rangle$ reveals that the non-linear response of the system to shear,

leading, *e.g.*, to shear thinning, is intimately related to the distribution of "local" microscopic shear stresses. We note that the potential energy per particle shows a similar time dependence as the local stress fluctuations.

Conclusions. – Extensive MD simulations have been used to elucidate the transient dynamics of a Yukawa mixture under shear. As a key to understand the non-linear response to shear fields, we have identified the stress relaxation after switching off the shear and its relation to the fluctuations of microscopic stresses. Whereas to a good approximation the average structure is not sufficient to distinguish a state in the elastic regime from one in the plastic-flow regime, the stress fluctuations are significantly larger in the latter case than in the former one. We have seen these transient phenomena for a deeply supercooled liquid and therefore they can be treated by MCT for glass-forming fluids under time-dependent shear [10,26]. Thus, our work provides a testing ground for the latter theory, in particular with respect to the relaxation of the shear stresses on the time scale $1/\dot{\gamma}$ after switching off the shear. We note that, at very low temperatures, the stress decay is a two-step process. Then, the decay on the time scale $1/\dot{\gamma}$ is followed by a second one which occurs on the intrinsic time scale of the unsheared system (*i.e.* a plateau is observed for the relaxation towards a glass) [27].

The sudden increase of local stress fluctuations around $\sigma_{\max}$ is in accordance with the recent identification of local irreversible events towards the plastic-flow regime. Here, we see that these events stem from a different distribution of local stresses in the sheared steady state from that in the elastic regime, the latter being similar to the distribution of local stresses at equilibrium. It is tempting to assume a direct relation between microscopic shear fluctuations and the effective temperature that has been estimated by Berthier *et al.* [15–17] studying the fluctuation-dissipation theorem for sheared systems. This is an issue for forthcoming studies.

* * *

We thank K. Binder, J. Brader, S. Egelhaaf, M. Fuchs, M. Laurati, F. Varnik, and T. Voigtmann for useful discussions. We are grateful to the DFG for financial support in the framework of the SFB TR6/A5. We acknowledge a substantial grant of CPU time at the NIC Jülich.

REFERENCES

[1] Larson R. G., *The Structure and Rheology of Complex Fluids* (Oxford University Press, New York) 1999.
[2] Lu J., Ravichandran G. and Johnson W. L., *Acta Mater.*, **51** (2003) 3429.
[3] Besseling R., Weeks E. R., Schofield A. B. and Poon W. C. K., *Phys. Rev. Lett.*, **99** (2007) 028301.
[4] Maloney C. E. and Lemaître A., *Phys. Rev. E*, **74** (2006) 016118.
[5] Tanguy A., Léonforte F. and Barrat J.-L., *Eur. Phys. J. E*, **20** (2006) 355.
[6] Tsamados M., Tanguy A., Léonforte F. and Barrat J.-L., *Eur. Phys. J. E*, **26** (2008) 283.
[7] Falk M. L. and Langer J. S., *Phys. Rev. E*, **57** (1998) 7192.
[8] Fuchs M. and Cates M. E., *Phys. Rev. Lett.*, **89** (2002) 248304.
[9] Fuchs M. and Cates M. E., *J. Phys.: Condens. Matter*, **17** (2005) S1681.
[10] Brader J. M., Voigtmann T., Cates M. E. and Fuchs M., *Phys. Rev. Lett.*, **98** (2007) 058301.
[11] Miyazaki K. and Reichman D. R., *Phys. Rev. E*, **66** (2002) 050501(R).
[12] Kobelev V. and Schweizer K. S., *Phys. Rev. E*, **71** (2005) 021401.
[13] Yamamoto R. and Onuki A., *Phys. Rev. E*, **58** (1998) 3515.
[14] Yamamoto R. and Onuki A., *Phys. Rev. Lett.*, **81** (1998) 4915.
[15] Berthier L., Barrat J.-L. and Kurchan J., *Phys. Rev. E*, **61** (2000) 5464.
[16] Berthier L. and Barrat J.-L., *Phys. Rev. Lett.*, **89** (2002) 095702.
[17] Berthier L. and Barrat J.-L., *J. Chem. Phys.*, **116** (2002) 6228.
[18] Miyazaki K., Reichman D. R. and Yamamoto R., *Phys. Rev. E*, **70** (2004) 011501.
[19] Varnik F. and Henrich O., *Phys. Rev. B*, **73** (2006) 174209.
[20] Varnik F., *J. Chem. Phys.*, **125** (2006) 164514.
[21] Rottler J. and Robbins M. O., *Phys. Rev. E*, **68** (2003) 011507.
[22] Rottler J. and Robbins M. O., *Phys. Rev. Lett.*, **95** (2005) 225504.
[23] Petikidis G., Vlassopoulos D. and Pusey P. N., *J. Phys.: Condens. Matter*, **16** (2004) S3955.
[24] Fuchs M. and Ballauff M., *J. Chem. Phys.*, **122** (2005) 094707.
[25] Krüger M. and Fuchs M., *Phys. Rev. Lett.*, **102** (2009) 135701.
[26] Zausch J., Horbach J., Laurati M., Egelhaaf S., Brader J.M., Voigtmann T. and Fuchs M., *J. Phys.: Condens. Matter*, **20** (2008) 404210.
[27] Zausch J., *Dynamics, Rheology and Critical Properties of Colloidal Fluid Mixtures* (Südwestdeutscher Verlag, Saarbrücken) 2009.
[28] Lees A. W. and Edwards S. F., *J. Phys. C: Solid State Phys.*, **5** (1972) 1921.
[29] Soddemann T., Dünweg B. and Kremer K., *Phys. Rev. E*, **68** (2003) 046702.
[30] Peters E. A. J. F., *Europhys. Lett.*, **66** (2004) 311.
[31] Binder K. and Kob W., *Glassy Materials and Disordered Solids: An Introduction to Their Statistical Mechanics* (World Scientific, Singapore) 2005.
[32] Hanley H. J. M., Rainwater J. C. and Hess S., *Phys. Rev. A*, **36** (1987) 1795.
[33] Gan H. H. and Eu B. C., *Phys. Rev. A*, **45** (1992) 3670.
[34] Abramowitz M. and Stegun I. A., *Handbook of Mathematical Functions* (Dover Publications, New York) 1972.
[35] Kabla A. and Debrégeas G., *Phys. Rev. Lett.*, **90** (2003) 258303.